RESEARCH ARTICLE - APPLIED GEOPHYSICS

Magnetic interpretation utilizing a new inverse algorithm for assessing the parameters of buried inclined dike-like geological structure

Khalid S. Essa[1] · Mahmoud Elhussein[1]

Abstract

A new algorithm has been established to interpret magnetic anomaly data due to inclined dike-like structure. This algorithm uses first horizontal derivative anomalies attained from magnetic anomaly data utilizing filters of sequential window lengths. The final estimated parameters are the half-width, the depth, angle of magnetization and amplitude factor of an inclined dike-like geological structure. A minimum variance criterion is used for selecting the most suitable variables. This algorithm has been realized to theoretical data without and with random noise. The effects of interference due to near structures have additionally been studied. The method was then applied to two field examples from Turkey and Peru, which demonstrate its effectiveness and accurateness. Thus, it is a respectable correspondence among the model parameters retrieved from this approach, drilling information, and the outcomes published in the literature. For example, in Turkey, we applied the technique to gauge the source variables and also the results were precise to $w = 64.74$ m and $h = 87.65$ m (2% and 3% errors, respectively) based on information from Aydin and Gelişli (Jeofizik 10:41–49, 1996).

Keywords Magnetic anomaly · Inclined dike · Depth · Half-width

Introduction

In magnetic elucidation problems, the anomalies owing to an inclined dike model have a wide use, e.g., oil, mineral, groundwater exploration and others (Smith et al. 2005; Abdelrahman et al. 2007a; Abdelrahman et al. 2012; Abo-Ezz and Essa 2016; Baiyegunhi and Gwavava 2017; Essa et al. 2018; Gadirov et al. 2018). However, in practice, an inclined dike configuration is often approximated by a vertical dike. This simple model may not be geologically accurate, but it is often times utilized in the geophysical interpretation to get the depth, width, and the thickness of a class of dike structures (Mehanee 2015; Mehanee and Essa 2015). Normal and rapid elucidation of such easy geometric models is administrated by hand through graphical approaches involving characteristic curves (Bean 1966; Koulomzine et al. 1970; Rao et al. 1972). However, the precision of the

estimated outcomes by these methods depends on the accuracy of the residual field separated from an observed field.

In addition, several numerical-approaches are adjusted to understand the magnetic anomaly caused by an inclined dike-like structure, such as curve matching techniques, which depend on trial and error of fitting the measured and calculated profile (Dondurur and Pamukçu 2003). Werner (1953) designed the deconvolution method (Werner deconvolution) to investigate inclined magnetized dikes by separating the anomaly owing to a selected dike from the interference of neighboring dikes. In spectral analysis approaches (Cassano and Rocca 1974; Sengupta and Das 1975; Bhimasankaram et al. 1978), the source depth is evaluated from the power band of their magnetic anomalies; the drawbacks of this method are that the precision of the outcomes is affected by the precision of the drawn interpolating line and it is difficult to apply this method when there are more than one body positioned at various depths (Cassano and Rocca 1974).

Rao et al. (1981) utilized a fancy gradient technique that depends on a few distinctive points (designated on the amplitude/phase plots) from which the variables of the dike are determined. Keating and Pilkington (1990) devised an

✉ Khalid S. Essa
 khalid_sa_essa@yahoo.com

1 Geophysics Department, Faculty of Science, Cairo University, Giza P.O. 12613, Egypt

automatic numerical routine to infer the vertical magnetic gradient profiles of an inclined dike. Abdelrahman et al. (2007b) suggested a semiautomatic least squares approach that convolves the inclined dike model with a moving average filter. However, the challenge facing this approach in estimating the model parameters is choosing the correct origin location of the dike from the measured magnetic data. Cooper (2012) discussed a new semiautomatic method to interpret the magnetic anomalies of dike by determining the fraction of the derivatives of the whole magnetic field. The disadvantage of this method is that it is applicable to thin dikes with different dips. Another method relies upon the amplitude of the analytic signal, which was devised by Cooper (2015) for the magnetic anomaly from a thin sheet to calculate the depth to the upper surface, amount of dip, and product of susceptibility and thickness of the dike. Al-Garni (2015) used a neural network method to estimate several parameters of dipping dikes. Essa and Elhussein (2017) discussed a semiautomatic method that depends on the second horizontal derivative of the measured magnetic anomaly for delineating dipping dikes sources. The shortcoming of the usage of higher order of derivatives is that sensitivity to noise is emphasized.

In this paper, we establish a new algorithm for calculating the response of an inclined dike model using the first derivative. The suggested method relies on evaluating the horizontal derivative anomalies from measured magnetic data utilizing several filters of successive window lengths (graticule spacings). The advantages of using this methodology are adjusted to estimate the depth and half-width of the covered inclined dike structures and also it is less sensitive to noise. The technique relies on calculating the variance (Var) of depths for every half-width. The tiniest variance is employed as a principle condition for deciding the most effective depth and half-width of the buried structure and does not need any graphical utilities. The accuracy of this methodology is demonstrated at synthetic examples, using simulated data generated from a model with random errors and a statistical distribution. The suggested method is then applied to real field examples from Turkey and Peru. There is an acceptable agreement between the results gained by our approach and those attained from different methods. Thus, the depths estimated from this approach are consistent with those attained from drilling information and published ones.
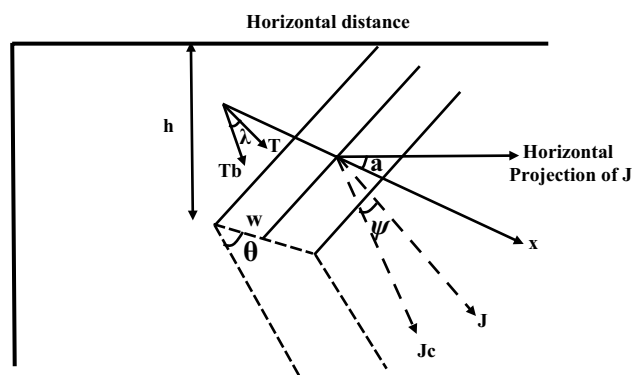

Fig. 1 A sketch diagram of inclined dike source

The method

Hood (1964), McGrath and Hood (1970) and Essa and Elhussein (2017) present an equation for the magnetic anomaly response of an inclined dike (Fig. 1) as follows:

$$
\begin{aligned}
H&(x_j, h, w, \theta) \\
&= A_c \Bigg[\sin\left(\theta \times \frac{\pi}{180}\right)\left(\tan^{-1}\left(\frac{x_j + w}{h}\right) - \tan^{-1}\left(\frac{x_j - w}{h}\right)\right) \\
&\quad - \frac{\cos\left(\theta \times \frac{\pi}{180}\right)}{2} \ln\left(\frac{(x_j + w)^2 + h^2}{(x_j - w)^2 + h^2}\right) \Bigg], \\
&\quad j = 1, 2, 3, 4, \ldots N
\end{aligned}
\tag{1}
$$

where h (m) is the depth to the upper surface of an inclined dike, w (m) is the half-width of the inclined dike, θ (°) is the angle of magnetization, x_j (m) are the horizontal coordinates of the observation points, and A_c (nT) is the amplitude factor related to magnetization.

Using the following three points $(x_j - s, x_j, x_j + s)$ on the anomaly profile, the first horizontal derivative (H_x) of the magnetic anomaly is given by subsequent expression:

$$
H_x(x_j, h, w, \theta, s) = \frac{H(x_j + s) - H(x_j - s)}{2s},
\tag{2}
$$

where $s = 1, 2, \ldots M$ spacing units which are called window lengths.

Substituting Eq. (1) in Eq. (2), the FHD (first horizontal derivative) of the magnetic anomaly is:

$$
\begin{aligned}
H_x&(x_j, h, w, \theta, s) \\
&= \frac{A_c}{2s} \Bigg[\sin\left(\theta \times \frac{\pi}{180}\right)\left(\tan^{-1}\left(\frac{x_j + s + w}{h}\right) + \tan^{-1}\left(\frac{-x_j - s + w}{h}\right) + \tan^{-1}\left(\frac{-x_j + s - w}{h}\right)\right. \\
&\quad \left. + \tan^{-1}\left(\frac{x_j - s - w}{h}\right)\right) + \frac{\cos\left(\theta \times \frac{\pi}{180}\right)}{2} \ln\left(\frac{\left(\frac{(x_j - s + w)^2 + h^2}{(x_j - s - w)^2 + h^2}\right)}{\left(\frac{(x_j + s + w)^2 + h^2}{(x_j + s - w)^2 + h^2}\right)}\right) \Bigg]
\end{aligned}
\tag{3}
$$

From the above equation and by rearrangement, we can gauge the depth (h_f), the half-width (w), the index angle (θ) and the amplitude factor (A_c) ("Appendix") as follows:

$$h_f = \frac{3s + w}{\tan\left(\frac{P}{q}\right)} \qquad (4)$$

where the factors P and q are defined in "Appendix".

$$\theta_c = \tan^{-1}\left[\frac{\frac{H_x(+s).\ln\left(\frac{(s-w)^2+h^2}{(s+w)^2+h^2}\right)}{H_x(0)} - \frac{1}{2}\ln\left(\frac{(2s-w)^2+h^2}{(2s+w)^2+h^2}\right)}{\tan^{-1}\left(\frac{2s+w}{h}\right) + \tan^{-1}\left(\frac{w-2s}{h}\right) + 2\tan^{-1}\left(\frac{-w}{h}\right)}\right]. \qquad (5)$$

$$A_c = \frac{2sH_x(0)}{\cos\theta \ln\left(\frac{(s-w)^2+h^2}{(s+w)^2+h^2}\right)}. \qquad (6)$$

The RMS (root-mean-square error) is estimated at various w values from the following equation:

$$\text{RMS} = \sqrt{\frac{\sum_{i=1}^{N}\left[H(x_j) - H_c(x_j)\right]^2}{N}}, \qquad (7)$$

where $H(x_j)$ is the measured field and $H_c(x_j)$ is the computed field. This is considered the misfit between the observed and calculated anomalies. The procedures and flowchart of applying our technique are summarized in Fig. 2.

The limitation of our method is based on: (a) the number of data points (larger than 21 points), (b) the convergence and stability of the minimizer, (c) a priori information accessible from different techniques that can be obtained as underlying model data.

Uncertainty analysis

We examined the uncertainties in estimating the model parameters (h, w, θ, A) of an inclined dike source by our method. For this purpose, each noise-free and noise-corrupted magnetic anomaly has been scrutinized and the impact of interference from neighboring bodies is considered.

Analysis of synthetic example

The total magnetic anomaly (ΔH) for an inclined dike with the parameters: $A_c = 1500$ nT, $\theta = 40°$, $h = 9$ m, $w = 4$ m, and profile length $= 100$ m, is

$$\Delta H(x_j)$$
$$= A_c\left[\left(\sin\left(40^o \times \frac{\pi}{180}\right)\right)\left(\tan^{-1}\left(\frac{x_j+4}{9}\right) - \tan^{-1}\left(\frac{x_j-4}{9}\right)\right)\right.$$
$$\left. - \frac{\cos\left(40^o \times \frac{\pi}{180}\right)}{2}\ln\left(\frac{(x_j+4)^2+9^2}{(x_j-4)^2+9^2}\right)\right]. \qquad (8)$$

Equation (2) is utilized to evaluate the horizontal derivative anomalies from the magnetic anomaly (ΔH) utilizing diverse s values ($s = 5, 6, 7, 8$ and 9 m). We estimated h
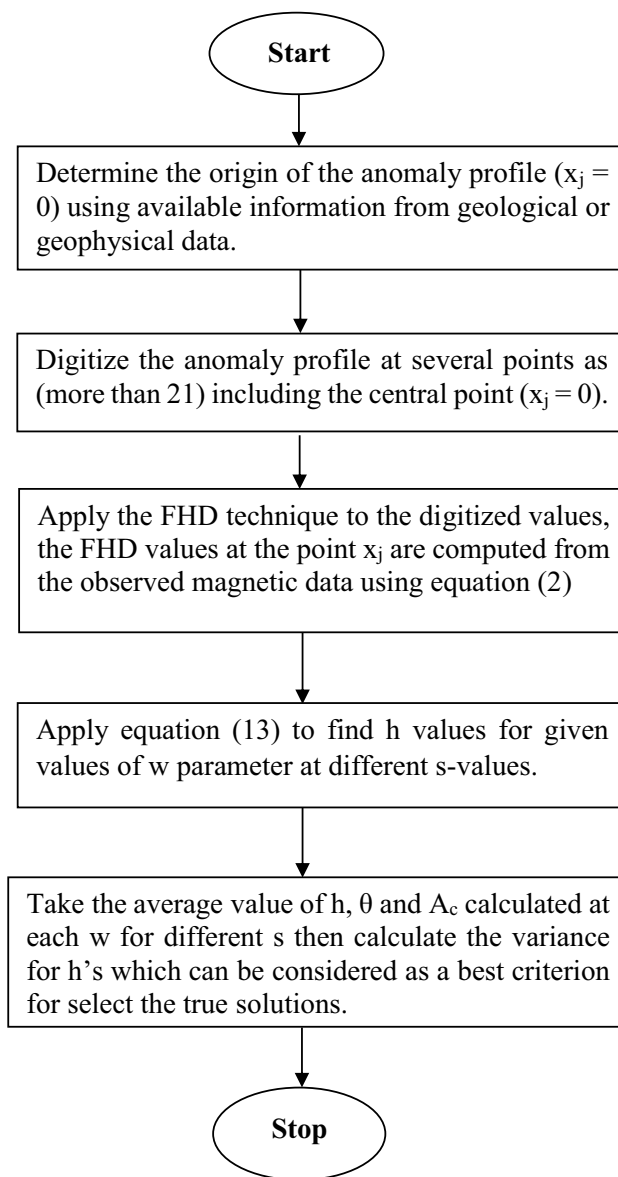

Fig. 2 Generalized scheme for parameters estimation by using our method

Table 1 Numerical results for a synthetic example with and without 10% random noise ($h = 9$ m, $\theta = 40°$, $A = 1500$ nT, $w = 4$ m, and profile length $= 100$ m)

w (m)	Parameters	s (m)					Average	Variance	RMS error (nT)
		5	6	7	8	9			
Without random noise									
2	h (m)	10.08	9.95	9.86	9.79	9.73	9.88	0.019	16.780
	θ (°)	40.03	39.82	39.63	39.50	39.41	39.68	0.062	
	A_c (nT)	3308.05	3243.50	3199.82	3167.38	3141.66	3212.08	4326.168	
2.5	h (m)	9.89	9.78	9.71	9.65	9.60	9.73	0.013	13.769
	θ (°)	40.03	39.85	39.69	39.59	39.52	39.73	0.043	
	A_c (nT)	2602.81	2559.89	2531.01	2509.59	2492.63	2539.19	1896.490	
3	h (m)	9.65	9.57	9.52	9.47	9.43	9.53	0.007	10.066
	θ (°)	40.02	39.89	39.77	39.69	39.64	39.80	0.023	
	A_c (nT)	2123.22	2096.83	2079.18	2066.14	2055.82	2084.24	709.624	
3.5	h (m)	9.36	9.31	9.28	9.26	9.23	9.29	0.002	5.499
	θ (°)	40.01	39.94	39.87	39.83	39.80	39.89	0.007	
	A_c (nT)	1771.97	1759.43	1751.10	1744.98	1740.15	1753.52	158.209	
4	h (m)	9.00	9.00	9.00	9.00	9.00	**9.00**	0.000	**0.000**
	θ (°)	40.00	40.00	40.00	40.00	40.00	**40.00**	0.000	
	A_c (nT)	1500.00	1500.00	1500.00	1500.00	1500.00	**1500.00**	0.000	
4.5	h (m)	8.57	8.63	8.67	8.70	8.73	8.66	0.004	6.622
	θ (°)	39.99	40.08	40.16	40.21	40.24	40.14	0.011	
	A_c (nT)	1279.78	1291.91	1299.78	1305.50	1310.01	1297.40	142.710	
5	h (m)	8.05	8.19	8.28	8.35	8.41	8.26	0.020	14.579
	θ (°)	39.97	40.19	40.36	40.47	40.53	40.30	0.053	
	A_c (nT)	1094.24	1118.92	1134.64	1146.00	1154.88	1129.74	574.383	
With 10% random noise									
2	h (m)	10.25	10.38	10.30	9.53	9.55	10.00	0.180	22.382
	θ (°)	40.17	39.89	37.51	41.59	39.47	39.73	2.169	
	A_c (nT)	3374.51	3408.67	3369.71	3015.63	3050.18	3243.74	37,417.392	
2.5	h (m)	10.07	10.21	10.15	9.38	9.42	9.85	0.168	20.016
	θ (°)	40.16	39.91	37.57	41.48	39.58	39.74	2.001	
	A_c (nT)	2655.82	2691.61	2666.48	2388.97	2419.82	2564.54	21,659.687	
3	h (m)	9.83	10.00	9.96	9.20	9.25	9.65	0.152	17.345
	θ (°)	40.15	39.93	37.43	41.40	39.71	39.73	2.071	
	$A_c A_c$ (nT)	2167.26	2206.18	2191.64	1966.41	1995.52	2105.40	13,202.675	
3.5	h (m)	9.54	9.75	9.73	8.99	9.05	9.41	0.135	14.510
	θ (°)	40.14	39.97	37.72	41.75	39.88	39.89	2.057	
	A_c (nT)	1809.56	1852.75	1847.06	1660.31	1688.84	1771.70	8238.740	
4	h (m)	9.19	9.34	9.45	8.73	8.81	**9.11**	0.103	**12.587**
	θ (°)	40.12	40.01	37.83	41.73	40.09	**39.95**	1.931	
	A_c (nT)	1532.81	1581.31	1583.55	1426.73	1455.50	**1515.98**	5184.879	
4.5	h (m)	8.77	9.08	9.13	8.42	8.24	8.73	0.155	13.154
	θ (°)	40.10	40.07	37.96	41.95	40.34	40.08	2.018	
	A_c (nT)	1328.88	1393.89	1373.68	1218.22	1230.85	1309.10	6533.090	
5	h (m)	8.35	8.66	8.75	8.02	8.11	8.38	0.105	14.301
	θ (°)	40.07	40.14	38.13	42.24	40.65	40.24	2.161	
	A_c (nT)	1150.44	1183.52	1284.84	1089.00	1120.05	1165.57	5677.898	

Bold represents the best-fit parmeters estimated

values at various w for each s value and afterward calculated the average depth and variance (Table 1) by using our inversion approach. Table 1 demonstrates the outcomes for noise-free data. The estimated parameters from the planned method are in fair agreement with the model of the 2D inclined dike ($h = 9$ m and $w = 4$ m). In the end, we can observe that the minimum variance (Var = 0) occurs at the true depth ($h = 9$ m) and true half-width ($w = 4$ m).

Subsequently, the real data are polluted with random noise; we imposed 10% random noise on the composite anomaly to see the impact of this noise on our algorithm. The FHD anomalies were computed using the same s values mentioned above.

Table 1 also shows the computational results for the noisy magnetic data. The average depth is 9.11 m, which is an error of 1.22% from the true h value and the estimated half-width is $w = 4$ m. The obtained solution for the different parameters corresponds to a minimum variance with an RMS which equal to 12.587 nT. This demonstrates that our method is valuable when applied to noisy magnetic data.

Analysis of the interference effect

The magnetic anomalies may be distorted due to nearby structures; a synthetic model composed of a 2D inclined dike (with $h = 9$ m, $\theta = 40°$, $A_c = 1500$ nT and $w = 4$ m) and a vertical thin dike (with $h = 4$ m, $\alpha = 45°$, $K = 2500$ nT and $x_o = 40$ m) was computed using a profile length of 120 m. The analysis by our method was applied to this synthetic data to evaluate and study the response of this neighboring structure on assessing the body parameters (h, w, θ and A_c) by using our new approach.

Figure 3 shows the composite magnetic anomaly due to the two structures with and without 10% random noise. The FHD technique was utilized to the magnetic anomaly without random noise using four graticule spacings ($s = 5, 6, 7$ and 8 m).

The values of h at several w for each s value were appraised by our method, and then the average and Var values of the different factors were calculated at various w for each s value (Table 2). From Table 2, the average depth of 8.33 m, w of 4.5 m, θ of 40.04° and A_c of 1208.03 nT correspond to the minimum RMS (RMS = 136.337 nT). The percentage error in depth is 7.44%, in half-width is 12.5%, in magnetization angle is 0.1% and in amplitude factor is 19.46%.

The FHD technique was repeated with 10% random noise for the same previous spacings ($s = 5, 6, 7$ and 8 m). From Table 2, the average depth h_c is 8.19 m, w is 4.5 m, θ_c is
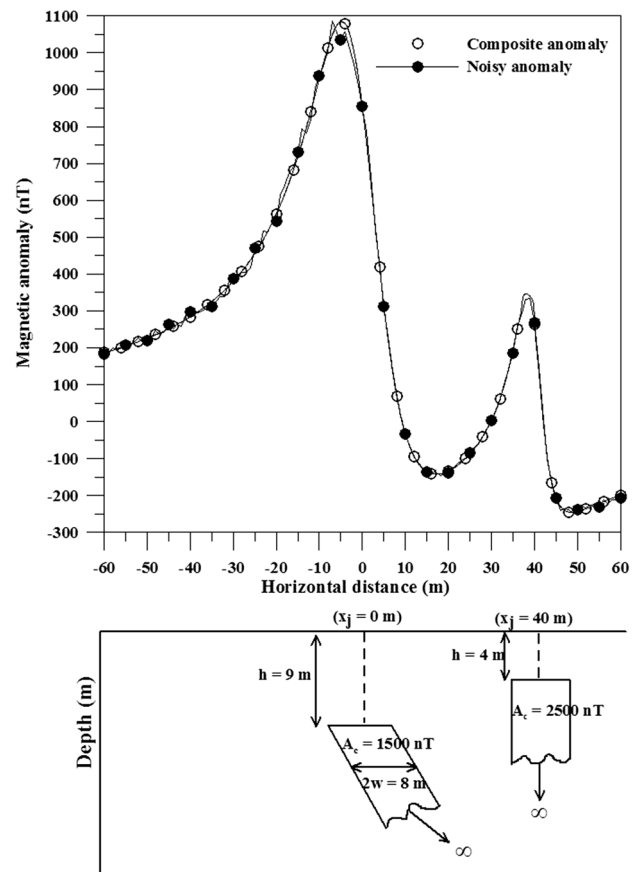
Fig. 3 A composite magnetic field anomaly of a buried inclined dike with $h = 9$ m, $\theta = 40°$, $A_c = 1500$ nT and $w = 4$ m, and a vertical thin dike with $h = 4$ m, $\alpha = 45°$, $K = 2500$ nT and $x_o = 40$ m, and profile length = 120 m with and without 10% random noise and a sketch diagram of the 2 sources

40.99° and A_c is 1176.46 nT; the corresponding minimum (RMS = 134.398 nT). The error of computed depth is 9% from the true depth (9 m), half-width is 12.5% from the true value (4 m), magnetization angle is 2.475% from the true value (40°); finally, the amplitude factor is 21.57% from the actual value (1500 nT).

Analysis of the effect of choosing origin

The selection of an incorrect origin of the magnetic profile from real data leads to errors in determining the inclined dike structure parameters. To determine the implication of choosing an incorrect origin, we used a synthetic model of $A_c = 1500$ nT, $\theta = 50°$, $h = 9$ m, $w = 4$ m, and profile length = 100 m) with an error (1.5 m) in the source location (see Eq. 9) as follows:

Table 2 Numerical results for a synthetic example composed of a 2D inclined dike (with $h=9$ m, $\theta=40°$, $A_c=1500$ nT and $w=4$ m), and a vertical dike (with $h=4$ m, $\alpha=45°$, $K=2500$ nT and $x_o=40$ m) with and without 10% random noise

w (m)	Parameters	s (m)				Average	Variance	RMS error (nT)
		5	6	7	8			
Without random noise								
2	h (m)	9.93	9.72	9.50	9.22	9.59	0.092	137.853
	θ (°)	40.00	39.73	39.46	39.15	39.59	0.131	
	A_c (nT)	3176.17	3073.87	2977.91	2872.04	3025.00	16,951.172	
2.5	h (m)	9.74	9.55	9.34	9.08	9.43	0.081	138.152
	θ (°)	39.99	39.77	39.54	39.26	39.64	0.099	
	A_c (nT)	2498.44	2425.31	2354.59	2274.55	2388.22	9192.195	
3	h (m)	9.50	9.33	9.15	8.89	9.22	0.068	138.609
	θ (°)	39.99	39.82	39.63	39.39	39.71	0.065	
	A_c (nT)	2037.46	1985.84	1933.35	1871.55	1957.05	5055.692	
3.5	h (m)	9.20	9.07	8.91	8.67	8.96	0.052	139.323
	θ (°)	39.98	39.88	39.75	39.56	39.79	0.033	
	A_c (nT)	1699.71	1665.47	1627.29	1579.48	1642.99	2667.185	
4	h (m)	8.84	8.76	8.62	8.41	8.66	0.036	140.333
	θ (°)	39.98	39.95	39.90	39.78	39.90	0.008	
	A_c (nT)	1438.07	1418.98	1392.86	1356.50	1401.60	1247.512	
4.5	h (m)	8.41	8.37	8.29	8.23	**8.33**	0.006	**136.337**
	θ (°)	39.97	40.06	40.10	40.04	**40.04**	0.003	
	A_c (nT)	1226.03	1221.09	1205.73	1179.263	**1208.03**	442.457	
5	h (m)	7.89	7.93	7.89	7.74	7.86	0.007	141.172
	θ (°)	39.96	40.19	40.34	40.37	40.22	0.036	
	A_c (nT)	1147.21	1156.39	1151.17	1087.69	1135.62	1034.965	
With 10% random noise								
2	h (m)	9.05	9.08	10.62	9.43	9.54	0.540	135.247
	θ (°)	44.41	42.05	36.29	39.46	40.55	12.164	
	A_c (nT)	2773.66	2800.02	3361.49	2936.05	2967.81	73,947.141	
2.5	h (m)	8.85	8.90	10.26	9.29	9.33	0.429	135.758
	θ (°)	44.41	42.10	36.34	39.56	40.60	12.015	
	A_c (nT)	2178.22	2207.29	2660.25	2325.65	2342.85	48,839.218	
3	h (m)	8.60	8.68	10.07	9.11	9.12	0.459	136.399
	θ (°)	44.42	42.17	36.41	39.68	40.67	11.830	
	A_c (nT)	1772.42	1805.25	2186.81	1914.02	1919.63	35,390.776	
3.5	h (m)	8.29	8.41	9.85	8.89	8.86	0.502	137.313
	θ (°)	44.43	42.26	36.49	39.84	40.76	11.609	
	A_c (nT)	1474.29	1511.73	1843.31	1615.79	1611.28	27,512.103	
4	h (m)	7.91	8.08	9.57	8.63	8.55	0.562	138.631
	θ (°)	44.45	42.37	36.59	40.04	40.86	11.353	
	A_c (nT)	1242.48	1285.46	1580.68	1388.16	1374.20	22,684.575	
4.5	h (m)	7.65	7.89	9.11	8.12	**8.19**	0.414	**134.398**
	θ (°)	44.38	42.52	36.76	40.28	**40.99**	10.727	
	A_c (nT)	1053.65	1103.32	1341.55	1207.32	**1176.46**	16,212.923	
5	h (m)	6.88	7.22	8.88	7.97	7.74	0.786	143.002
	θ (°)	44.52	42.72	36.89	40.58	41.18	10.759	
	A_c (nT)	893.17	951.11	1199.41	1058.88	1025.64	18,134.564	

Bold represents the best-fit parmeters estimated

Table 3 Numerical results for a synthetic example composed of a 2D inclined dike (with $h=9$ m, $\theta=50°$, $A_c=1500$ nT and $w=4$ m), with incorrect origin

| w (m)	Parameters	s (m)				Average	Variance	RMS error (nT)
		5	6	7	8			
2	h (m)	9.25	9.06	8.91	8.79	9.00	0.038	88.894
	θ (°)	57.07	55.83	54.38	52.86	55.04	3.317	
	A_c (nT)	3122.66	3040.55	2982.16	2938.89	3021.06	6322.521	
2.5	h (m)	9.05	8.88	8.75	8.64	8.83	0.031	87.734
	θ (°)	57.06	55.86	54.44	52.95	55.08	3.152	
	A_c (nT)	2452.09	2396.34	2356.67	2327.48	2383.15	2909.129	
3	h (m)	8.80	8.66	8.55	8.46	8.62	0.022	86.464
	θ (°)	57.04	55.89	54.52	53.07	55.13	2.946	
	A_c (nT)	1995.06	1959.30	1933.78	1915.10	1950.81	1198.323	
3.5	h (m)	8.50	8.39	8.30	8.23	8.35	0.013	85.357
	θ (°)	57.01	55.93	54.62	53.21	55.19	2.696	
	A_c (nT)	1659.33	1640.15	1626.27	1616.27	1635.50	348.218	
4	h (m)	8.12	8.06	8.01	7.97	**8.04**	0.004	**83.692**
	θ (°)	56.28	55.99	54.75	53.60	**55.15**	1.513	
	A_c (nT)	1398.38	1394.07	1390.47	1388.12	**1392.76**	20.004	
4.5	h (m)	7.64	7.66	7.79	7.62	7.68	0.006	84.439
	θ (°)	56.94	56.07	54.92	53.63	55.39	2.061	
	A_c (nT)	1185.92	1195.94	1202.01	1206.78	1197.66	80.937	
5	h (m)	7.11	7.19	7.24	7.28	7.21	0.005	85.765
	θ (°)	56.90	56.18	55.14	53.92	55.53	1.674	
	A_c (nT)	1005.60	1030.32	1046.05	1057.85	1034.96	510.024	

Bold represents the best-fit parmeters estimated

$$\Delta H(x_i) = A_c \left[\left(\sin\left(50° \times \frac{\pi}{180}\right) \right) \left(\tan^{-1}\left(\frac{(x_j - 1.5) + 4}{9} \right) \right. \right.$$

$$\left. - \tan^{-1}\left(\frac{(x_j - 1.5) - 4}{9} \right) \right) - \frac{\cos\left(50° \times \frac{\pi}{180}\right)}{2}$$

$$\left. \times \ln\left(\frac{((x_j - 1.5) + 4)^2 + 9^2}{((x_j - 1.5) - 4)^2 + 9^2} \right) \right].$$

(9)

Our investigation begins by utilizing Eq. (2) for the FHD separation anomalies from the magnetic anomaly (ΔH) using available s values ($s=5$, 6, 7 and 8 m).

Table 3 displays the results after applying the error in the horizontal coordinate. The estimated parameters (h, w, θ and A_c) are 8.04 m, 4 m, 55.15° and 1392.76 nT, respectively, and correspond to the minimum RMS of 83.692 nT. The error in computed depth is 10.66%, in half-width is 0%, in index parameter is 10.3% while the error of estimated amplitude factor is 7.15%.
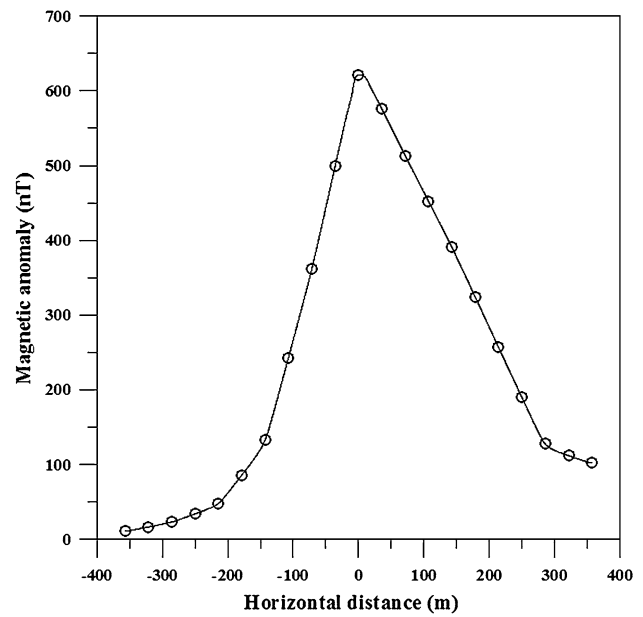
Fig. 4 A vertical component magnetic anomaly Bayburt–Sarihan (northeast of Turkey) skarn dike by Dondurur and Pamukçu (2003)

Field examples

To test the validity and the rationality of the anticipated approach, we have explored two real field cases with increasing complexity of the geological sources collected from the available published literature.

Magnetic anomaly of the Bayburt–Sarihan skarn zone, Turkey

A vertical component magnetic field profile was taken over the Bayburt–Sarihan (northeast of Turkey) skarn dike by Dondurur and Pamukçu (2003) (Fig. 4). The length of this profile is 714.5 m, and it was digitized at 8.93 m sample interval. We have applied our new technique to determine the body parameters (z, d) using five successive windows

$(s = 62.51, 71.44, 80.37, 89.3,$ and 98.23 m) for the horizontal derivative anomalies. Table 4 shows that the parameters with the best-fit parameters are: $w = 64.74$ m, $h = 87.65$ m, $\theta = -71.37°$ and $A_c = -409.25$ nT (RMS = 69.353). Table 5 shows the comparison with other interpretation methods from the published literature.

Magnetic anomaly in the Marcona district, Peru

The magnetic field profile taken by Gay (1963) near the magnetic equator in the Marcona district, Peru, is shown in Fig. 5. The profile length is 1125 m and was digitized at 14.06 m. Following the previous outlined process, the horizontal derivative anomalies were calculated from Eq. (2) by using seven s value ($s = 126.54, 140.6, 154.66, 168.72, 182.78, 196.84$ and 210.9 m). For our algorithm,

Table 4 Numerical results for Bayburt–Sarihan (northeast of Turkey) skarn zone field example
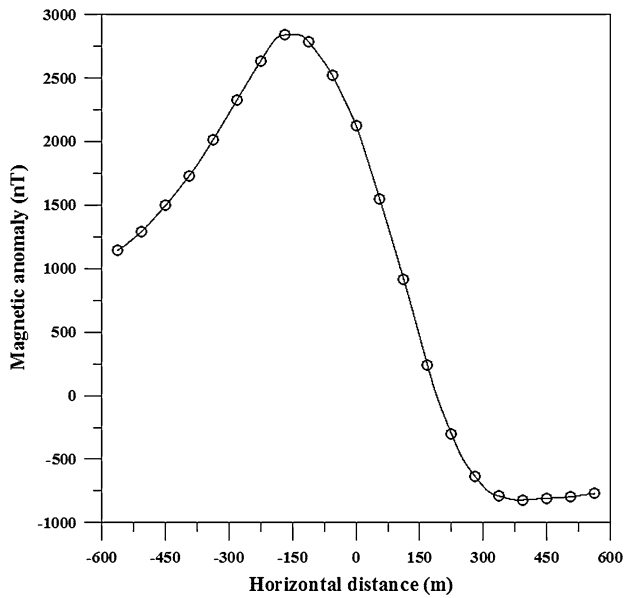
w (m)	Parameters	s (m)					Average	Variance	RMS error (nT)
		62.51	71.44	80.37	89.3	98.23			
62.51	h (m)	−71.44	−71.19	−71.31	−71.49	−71.46	90.62	221.299	70.726
	θ (°)	−71.44	−71.19	−71.31	−71.49	−71.46	−71.38	0.016	
	A_c (nT)	−297.61	−362.74	−438.02	−518.46	−574.60	−438.29	12,626.513	
64.74	h (m)	67.44	78.70	89.65	99.85	102.63	**87.65**	216.427	**69.353**
	θ (°)	−71.38	−71.21	−71.30	−71.49	−71.46	**−71.37**	0.013	
	A_c (nT)	−277.08	−341.67	−415.35	−493.68	−518.49	**−409.25**	10,283.907	
66.98	h (m)	63.74	75.84	87.29	97.83	103.81	85.70	264.218	76.328
	θ (°)	−71.32	−71.13	−71.28	−71.48	−71.46	−71.33	0.020	
	A_c (nT)	−256.98	−321.38	−393.73	−470.17	−523.82	−393.22	11,675.083	
69.21	h (m)	59.60	72.74	84.77	95.68	101.90	82.94	293.448	79.520
	θ (°)	−71.24	−71.10	−71.27	−71.48	−71.46	−71.31	0.025	
	A_c (nT)	−237.06	−301.74	−373.02	−447.81	−500.41	−372.01	11,345.857	
71.44	h (m)	54.88	69.34	82.07	93.41	99.88	79.92	330.915	83.035
	θ (°)	−71.15	−71.06	−71.25	−71.47	−71.46	−71.28	0.034	
	A_c (nT)	−216.96	−282.57	−353.10	−426.45	−478.14	−351.44	11,127.507	
73.67	h (m)	49.32	65.60	79.16	90.99	97.75	76.57	381.454	86.962
	θ (°)	−71.04	−71.02	−71.24	−71.47	−71.47	−71.25	0.048	
	A_c (nT)	−196.10	−263.68	−333.82	−405.96	−456.88	−331.29	11,050.705	

Bold represents the best-fit parmeters estimated

Table 5 Comparison between numerical results of different methods for Bayburt–Sarihan (northeast of Turkey) skarn zone field example

Parameters	Method					
	Aydin and Gelişlli method (1996)	Dondurur and Pamukçu method (2003)			Abdelrahman et al. method (2007b)	Present method
		Inverse solution	Hilbert transform	Power spectrum		
h_{averg} (m)	94	97	100	98	100	87.65
w (m)	66	76	75	70	79	64.74
θ (°)	–	–	–	–	–	−71.37
A_c (nT)	–	–	–	–	–	−409.25

Fig. 5 Observed magnetic anomaly near the magnetic equator at Marcona district, Peru (Gay 1963)

the retrieved parameters are as follows: $h = 138.28$ m, $w = 196.84$ m, $\theta = 40.49°$ and $A_c = 1862.75$ nT which are the best-fit model parameters (RMS = 48.5567 nT) (Table 6). The estimated results from our process are in sensible agreement with those published in the literature (Table 7).

Conclusions

The estimation of the parameters of an inclined dike are very important in geophysical exploration. We have devised an algorithm, which is based on the first horizontal derivative technique to gauge the body parameters. Our new approach is easy, semiautomatic and it does not necessitate any graphical supports. To verify the accurateness and pertinence of our method, the approach has been applied to synthetic data without and with random noise, and applied it also to a more complicated synthetic model including interference effect, again with and without random noise.

From our outcomes, we show that the best-fit parameters for the inclined dike can be determined with reasonable accuracy from our new algorithm even if the observed data are tainted with noise. Furthermore, the method has been

Table 6 Numerical results for Marcona district field example, Peru

w (m)	Parameters	s (m)							Average	Variance	RMS error (nT)
		126.54	140.6	154.66	168.72	182.78	196.84	210.9			
182.78	h (m)	162.75	161.89	161.78	169.32	171.39	218.26	264.72	187.16	1571.434	167.75
	θ (°)	43.25	42.90	42.78	41.40	40.27	37.45	35.45	40.50	9.029	
	A_c (nT)	2015.96	2001.90	2012.43	2084.94	2104.35	2581.12	3075.90	2268.09	168,446.901	
186.295	h (m)	151.30	152.95	154.12	162.74	165.46	213.67	260.92	180.17	1735.987	147.413
	θ (°)	43.01	42.83	42.83	41.52	40.44	37.54	35.50	40.53	8.664	
	A_c (nT)	1872.86	1889.78	1915.10	1996.94	2023.01	2498.11	2987.91	2169.10	176,661.701	
189.81	h (m)	138.10	143.06	145.75	155.64	159.12	208.87	256.97	172.50	1947.912	124.877
	θ (°)	42.67	42.74	42.90	41.66	40.64	37.64	35.55	40.54	8.253	
	A_c (nT)	1722.36	1775.31	1816.74	1908.94	1942.11	2416.72	2902.14	2069.19	187,800.103	
193.325	h (m)	122.55	131.94	136.48	147.94	152.29	203.82	252.87	163.98	2230.391	100.424
	θ (°)	42.15	42.62	42.98	41.83	40.88	37.74	35.61	40.54	7.791	
	A_c (nT)	1561.62	1657.20	1716.34	1820.29	1861.19	2336.77	2818.42	1967.40	202,915.960	
196.84	h (m)	103.96	119.25	116.08	129.50	134.93	159.58	204.68	**138.28**	1163.967	**48.5567**
	θ (°)	41.26	42.43	43.07	42.03	41.15	37.86	35.67	**40.49**	7.327	
	A_c (nT)	1588.76	1533.68	1612.39	1730.15	1779.66	2258.01	2536.59	**1862.75**	146,803.465	
200.355	h (m)	82.56	104.36	113.95	129.98	136.71	192.94	244.17	143.52	3154.515	49.782
	θ (°)	39.60	42.12	43.19	42.27	41.47	37.49	35.73	40.27	7.700	
	A_c (nT)	1211.73	1402.29	1502.24	1637.19	1696.66	2180.25	2656.48	1755.26	249,038.578	
203.87	h (m)	62.28	86.38	99.06	119.06	127.55	187.03	239.55	131.56	3801.377	51.463
	θ (°)	36.75	41.55	43.36	42.60	41.88	38.13	35.80	40.01	9.285	
	A_c (nT)	1063.55	1259.95	1379.91	1539.05	1610.86	2103.22	2577.95	1647.78	274,887.994	

Bold represents the best-fit parmeters estimated

Table 7 Comparison between numerical results of different methods for Marcona district field example, Peru

Parameters	Method					
	Gay method (1963)	Koulomzine et al. method (1970)		Pal method (1985)	Al-Garni method (2015)	Present method
		With (φ)	With (μ)			
h_{averg} (m)	124	126.7	135.5	132.6	130	138.28
w (m)	186	205.95	202.75	193.75	191.7	196.84
θ (°)	–	–	–	–	–	40.49
A_c (nT)	–	–	–	–	–	1862.75

relevantly applied to two field data from Turkey and Peru, obtained over mineral rich deposits. The limitation of our approach concerns the convergence of s-values, i.e., not all s-values can give results. The good agreement of the results acquired from our method with those published in the literature shows that the inclined dike parameters can be reasonably and efficiently determined.

Appendix

Hood (1964), McGrath and Hood (1970) and Essa and Elhussein (2017) represent an equation for the total magnetic anomaly of an inclined dike (Fig. 1) as follows:

$$H(x_j, h, w, \theta)$$
$$= A_c \left[\sin \left(\theta \times \frac{\pi}{180} \right) \left(\tan^{-1} \left(\frac{x_j + w}{h} \right) - \tan^{-1} \left(\frac{x_j - w}{h} \right) \right) \right.$$
$$\left. - \frac{\cos \left(\theta \times \frac{\pi}{180} \right)}{2} \ln \left(\frac{(x_j + w)^2 + h^2}{(x_j - w)^2 + h^2} \right) \right],$$
$$j = 1, 2, 3, 4, \dots N \tag{10}$$

where h (m) is the depth to the top of the inclined dike, w (m) is the half-width of the inclined dike, θ (°) is the angle of magnetization (index parameter), x_j (m) are the horizontal coordinates, and A (nT) is the amplitude factor.

Using three observation points ($x_j - s, x_j, x_j + s$) along the anomaly profile; the first horizontal derivative (H_x) of the total magnetic anomaly is given by the following expression:

$$H_x(x_j, h, w, \theta, s) = \frac{H(x_j + s) - H(x_j - s)}{2s}, \tag{11}$$

where $s = 1, 2, \dots M$ spacing units which is called the graticule spacing or window length.

Substituting Eq. (10) in Eq. (11), the first horizontal derivative (FHD) of the total magnetic anomaly is given by:

$$H_x(x_j, h, w, \theta, s)$$
$$= \frac{A_c}{2s} \left[\sin \left(\theta \times \frac{\pi}{180} \right) \left(\tan^{-1} \left(\frac{x_j + s + w}{h} \right) \right. \right.$$
$$+ \tan^{-1} \left(\frac{-x_j - s + w}{h} \right)$$
$$+ \tan^{-1} \left(\frac{-x_j + s - w}{h} \right) + \tan^{-1} \left(\frac{x_j - s - w}{h} \right) \right)$$
$$+ \frac{\cos \left(\theta \times \frac{\pi}{180} \right)}{2} \ln \left(\frac{\left(\frac{(x_j - s + w)^2 + h^2}{(x_j - s - w)^2 + h^2} \right)}{\left(\frac{(x_j + s + w)^2 + h^2}{(x_j + s - w)^2 + h^2} \right)} \right) \right]. \tag{12}$$

By substituting $x_j = 0$ in Eq. (12), the amplitude factor (A_c) can be estimated as follows when $s > w$:

$$A_c = \frac{2s H_x(0)}{\cos \left(\theta \times \frac{\pi}{180} \right) \ln \left(\frac{(s-w)^2 + h^2}{(s+w)^2 + h^2} \right)}. \tag{13}$$

Using Eq. (13), Eq. (12) can be written as the follows:

$$H_x(x_j, h, w, \theta, s)$$
$$= \frac{H_x(0)}{\cos \left(\theta \times \frac{\pi}{180} \right) \ln \left(\frac{(s-w)^2 + h^2}{(s+w)^2 + h^2} \right)}$$
$$\times \left[\sin \left(\theta \times \frac{\pi}{180} \right) \left(\tan^{-1} \left(\frac{x_j + s + w}{h} \right) \right. \right.$$
$$+ \tan^{-1} \left(\frac{-x_j - s + w}{h} \right)$$
$$+ \tan^{-1} \left(\frac{-x_j + s - w}{h} \right) + \tan^{-1} \left(\frac{x_j - s - w}{h} \right) \right)$$
$$+ \frac{\cos \theta}{2} \ln \left(\frac{\left(\frac{(x_j - s + w)^2 + h^2}{(x_j - s - w)^2 + h^2} \right)}{\left(\frac{(x_j + s + w)^2 + h^2}{(x_j + s - w)^2 + h^2} \right)} \right) \right] \tag{14}$$

Putting $x_j = +s$, $x_j = -s$, $x_j = +2s$, $x_j = -2s$, we get the following four equations, respectively:

$H_x(+s)$

$$= \frac{H_x(0)}{\cos\left(\theta \times \frac{\pi}{180}\right) \ln\left(\frac{(s-w)^2+h^2}{(s+w)^2+h^2}\right)}$$

$$\times \left[\sin\left(\left(\theta \times \frac{\pi}{180}\right) \times \frac{\pi}{180}\right)\left(\tan^{-1}\left(\frac{2s+w}{h}\right)\right.\right.$$

$$\left. + \tan^{-1}\left(\frac{w-2s}{h}\right) + 2\tan^{-1}\left(-\frac{w}{h}\right)\right)$$

$$\left. + \frac{\cos\left(\theta \times \frac{\pi}{180}\right)}{2} \ln\left(\frac{(2s-w)^2+h^2}{(2s+w)^2+h^2}\right) \right] \quad (15)$$

$$H_x(-s) = \frac{H_x(0)}{\cos\left(\theta \times \frac{\pi}{180}\right) \ln\left(\frac{(s-w)^2+h^2}{(s+w)^2+h^2}\right)}$$

$$\times \left[\sin\left(\theta \times \frac{\pi}{180}\right)\left(2\tan^{-1}\left(\frac{w}{h}\right)\right.\right.$$

$$\left. + \tan^{-1}\left(\frac{2s-w}{h}\right) + \tan^{-1}\left(\frac{-2s-w}{h}\right)\right)$$

$$\left. + \frac{\cos\left(\theta \times \frac{\pi}{180}\right)}{2} \ln\left(\frac{(2s-w)^2+h^2}{(2s+w)^2+h^2}\right) \right] \quad (16)$$

$$H_x(+2s) = \frac{H_x(0)}{\cos\left(\theta \times \frac{\pi}{180}\right) \ln\left(\frac{(s-w)^2+h^2}{(s+w)^2+h^2}\right)}$$

$$\times \left[\sin\left(\theta \times \frac{\pi}{180}\right)\left(\tan^{-1}\left(\frac{3s+w}{h}\right)\right.\right.$$

$$+ \tan^{-1}\left(\frac{w-3s}{h}\right) + \tan^{-1}\left(\frac{-s-w}{h}\right)$$

$$\left. + \tan^{-1}\left(\frac{s-w}{h}\right)\right) + \frac{\cos\left(\theta \times \frac{\pi}{180}\right)}{2}$$

$$\left. \times \ln\left(\frac{\left(\frac{(s+w)^2+h^2}{(s-w)^2+h^2}\right)}{\left(\frac{(3s+w)^2+h^2}{(3s-w)^2+h^2}\right)}\right) \right] \quad (17)$$

$H_x(-2s)$

$$= \frac{H_x(0)}{\cos\left(\theta \times \frac{\pi}{180}\right) \ln\left(\frac{(s-w)^2+h^2}{(s+w)^2+h^2}\right)}$$

$$\left[\sin\left(\theta \times \frac{\pi}{180}\right)\left(\tan^{-1}\left(\frac{w-s}{h}\right) + \tan^{-1}\left(\frac{s+w}{h}\right)\right.\right.$$

$$\left. + \tan^{-1}\left(\frac{3s-w}{h}\right) + \tan^{-1}\left(\frac{-3s-w}{h}\right)\right)$$

$$\left. + \frac{\cos\left(\theta \times \frac{\pi}{180}\right)}{2} \ln\left(\frac{\left(\frac{(3s-w)^2+h^2}{(3s+w)^2+h^2}\right)}{\left(\frac{(s-w)^2+h^2}{(s+w)^2+h^2}\right)}\right) \right] \quad (18)$$

By subtracting Eq. (16) from Eq. (15) and Eq. (18) from Eq. (17), we get the following two equations, respectively:

$H_x(+s) - H_x(-s)$

$$= \frac{H_x(0) \sin\left(\theta \times \frac{\pi}{180}\right)}{\cos\left(\theta \times \frac{\pi}{180}\right) \ln\left(\frac{(s-w)^2+h^2}{(s+w)^2+h^2}\right)}$$

$$\times \left[2\tan^{-1}\left(\frac{2s+w}{h}\right) + 2\tan^{-1}\left(\frac{w-2s}{h}\right) + 4\tan^{-1}\left(-\frac{w}{h}\right) \right] \quad (19)$$

$H_x(+2s) - H_x(-2s)$

$$= \frac{H_x(0) \sin\left(\theta \times \frac{\pi}{180}\right)}{\cos\left(\theta \times \frac{\pi}{180}\right) \ln\left(\frac{(s-w)^2+h^2}{(s+w)^2+h^2}\right)} \quad (20)$$

$$\left[2\tan^{-1}\left(\frac{3s+w}{h}\right) + 2\tan^{-1}\left(\frac{w-3s}{h}\right) \right.$$

$$\left. + 2\tan^{-1}\left(\frac{-s-w}{h}\right) + 2\tan^{-1}\left(\frac{s-w}{h}\right) \right]$$

Then by dividing Eq. (19) by Eq. (20), we get the following:

$$q = \frac{\tan^{-1}\left(\frac{2s+w}{h}\right) + \tan^{-1}\left(\frac{w-2s}{h}\right) + 2\tan^{-1}\left(-\frac{w}{h}\right)}{\tan^{-1}\left(\frac{3s+w}{h}\right) + \tan^{-1}\left(\frac{w-3s}{h}\right) + \tan^{-1}\left(\frac{-s-w}{h}\right) + \tan^{-1}\left(\frac{s-w}{h}\right)}, \quad (21)$$

where

$$q = \frac{H_x(+s) - H_x(-s)}{H_x(+2s) - H_x(-2s)}.$$

From Eq. (21) and by rearrangement, we can calculate h_f from the following equation:

$$h_f = \frac{3s + w}{\tan\left(\frac{P}{q}\right)},$$ (22)

where

$$P = q\tan^{-1}\left(\frac{3s - w}{h_i}\right) + q\tan^{-1}\left(\frac{s + w}{h_i}\right) + q\tan^{-1}\left(\frac{w - s}{h_i}\right)$$
$$+ \tan^{-1}\left(\frac{2s + w}{h_i}\right) + \tan^{-1}\left(\frac{w - 2s}{h_i}\right) + 2\tan^{-1}\left(-\frac{w}{h_i}\right).$$

Equation (22) can be deciphered for h using the standard methods for solving nonlinear equations (Press et al. 1986), and its iteration form can be expressed as:

$$h_f = f(h_i),$$ (23)

where h_i is the initial depth estimate and h_f is the revised depth, for the next iteration h_f will be used as h_i. The iteration stops when $|h_f - h_i| \le e$, where e is a small predetermined real number close to zero.

From Eq. (15), we can calculate the magnetization angle as follows:

$$\theta c = \tan^{-1}\left[\frac{\frac{H_x(+s).\ln\left(\frac{(s-w)^2 + h^2}{(s+w)^2 + h^2}\right)}{M_x(0)} - \frac{1}{2}\ln\left(\frac{(2s-w)^2 + h^2}{(2s+w)^2 + h^2}\right)}{\tan^{-1}\left(\frac{2s+w}{h}\right) + \tan^{-1}\left(\frac{w-2s}{h}\right) + 2\tan^{-1}\left(\frac{-w}{h}\right)}\right].$$ (24)

References

Abdelrahman EM, Abo-Ezz ER, Essa KS, El-Araby TM, Soliman KS (2007a) A new least-squares minimization approach to depth and shape determination from magnetic data. Geophys Prospect 55:433–446

Abdelrahman EM, Abo-Ezz ER, Soliman KS, EL-Araby TM, Essa KS (2007b) A least-squares window curves method for interpretation of magnetic anomalies caused by dipping dikes. Pure Appl Geophys 164:1027–1044

Abdelrahman EM, Abo-Ezz ER, Essa KS (2012) Parametric inversion of residual magnetic anomalies due to simple geometric bodies. Explor Geophys 43:178–189

Abo-Ezz ER, Essa KS (2016) A least-squares minimization approach for model parameters estimate by using a new magnetic anomaly formula. Pure Appl Geophys 173:1265–1278

Al-Garni MA (2015) Interpretation of magnetic anomalies due to dipping dikes using neural network inversion. Arab J Geosci 8:8721–8729

Aydin A, Gelişli K (1996) Magnetic studies for the skarn zone of Sarihan-Bayburt. Jeofizik 10:41–49 **(in Turkish with English Abstract)**

Baiyegunhi C, Gwavava O (2017) Magnetic investigation and 2 D gravity profile modelling across the Beattie magnetic anomaly in the southeastern Karoo Basin, South Africa. Acta Geophys 65:119–138

Bean RJ (1966) A rapid graphical solution for the aeromagnetic anomaly of the two-dimensional tabular body. Geophysics 31:963–970

Bhimasankaram VLS, Mohan NI, Seshagiri Rao SV (1978) Interpretation of magnetic anomalies of dikes using Fourier transforms. Geophys Explor 16:259–266

Cassano E, Rocca F (1974) Interpretation of magnetic anomalies using spectral estimation techniques. Geophys Prospect 23:663–681

Cooper GRJ (2012) The semi-automatic interpretation of magnetic dyke anomalies. Comput Geosci 44:95–99

Cooper GRJ (2015) Using the analytic signal amplitude to determine the location and depth of thin dikes from magnetic data. Geophysics 80:1–6

Dondurur D, Pamukçu OA (2003) Interpretation of magnetic anomalies from dipping dike model using inverse solution, power spectrum and Hilbert transform methods. J Balk Geophys Soc 6:127–139

Essa KS, Elhussein M (2017) A new approach for the interpretation of magnetic data by a 2-D dipping dike. J Appl Geophys 136:431–443

Essa KS, Nady AG, Mostafa MS, Elhussein M (2018) Implementation of potential field data to depict the structural lineaments of the Sinai Peninsula, Egypt. J Afr Earth Sci 147:43–53

Gadirov VG, Eppelbaum LV, Kuderavets RS, Menshove OI, Gadirov KV (2018) Indicative features of local magnetic anomalies from hydrocarbon deposits: examples from Azerbaijan and Ukraine. Acta Geophys. https://doi.org/10.1007/s11600-018-0224-0

Gay SP (1963) Standard curves for interpretation of magnetic anomalies over long tabular bodies. Geophysics 28:161–200

Hood P (1964) The Königsberger ratio and the dipping-dyke equation. Geophys Prospect 12:440–456

Keating PB, Pilkington M (1990) An automated method for the interpretation of magnetic vertical-gradient anomalies. Geophysics 55:336–343

Koulomzine T, Lamontagne Y, Nadeau A (1970) New methods for the direct interpretation of magnetic anomalies caused by inclined dikes of infinite length. Geophysics 35:812–830

McGrath PH, Hood PJ (1970) The dipping dike case, a computer curve matching method of magnetic interpretation. Geophysics 35:831–848

Mehanee SA (2015) Tracing of paleo-shear zones by self-potential data inversion: case studies from the KTB, Rittsteig, and Grossensees graphite-bearing fault planes. Earth Planets Space 67(1):14

Mehanee SA, Essa KS (2015) 2.5D regularized inversion for the interpretation of residual gravity data by a dipping thin sheet: numerical examples and case studies with an insight on sensitivity and non-uniqueness. Earth Planets Space 67(1):130

Pal PC (1985) A gradient analysis based simplified inversion strategy for the magnetic anomaly of an inclined and infinite thick dike. Geophysics 50:1179–1182

Press WH, Flannery BP, Teukolsky SA, Vetterling WT (1986) Numerical recipes, the art of scientific computing. Cambridge University Press, Cambridge

Rao BSR, Prakasa Rao TKS, Gopala Rao D, Kesavamani M (1972) Derivatives and dike anomaly interpretation. Pure Appl Geophys 99:120–129

Rao DA, Babu HVR, Narayan PVS (1981) Interpretation of magnetic anomalies due to dikes: the complex gradient method. Geophysics 46:1572–1578

Sengupta S, Das SK (1975) Interpretation of magnetic anomalies of dikes by Fourier transforms. Pure Appl Geophys 113:625–633

Smith RS, Salem A, Lemieux J (2005) An enhanced method for source parameter imaging of magnetic data collected for mineral exploration. Geophys Prospect 53:655–665

Werner S (1953) Interpretation of magnetic anomalies of sheet-like bodies. Sveriges Geologiska Undersökning. Ser C Årsbok 43(6):49